

Optimization of wire electrical discharge machining (WEDM) process parameters using Taguchi method

S. S. Mahapatra · Amar Patnaik

Abstract Wire electrical discharge machining (WEDM) is extensively used in machining of conductive materials when precision is of prime importance. Rough cutting operation in WEDM is treated as a challenging one because improvement of more than one machining performance measures viz. metal removal rate (MRR), surface finish (SF) and cutting width (kerf) are sought to obtain a precision work. Using Taguchi's parameter design, significant machining parameters affecting the performance measures are identified as discharge current, pulse duration, pulse frequency, wire speed, wire tension, and dielectric flow. It has been observed that a combination of factors for optimization of each performance measure is different. In this study, the relationship between control factors and responses like MRR, SF and kerf are established by means of nonlinear regression analysis, resulting in a valid mathematical model. Finally, genetic algorithm, a popular evolutionary approach, is employed to optimize the wire electrical discharge machining process with multiple objectives. The study demonstrates that the WEDM process parameters can be adjusted to achieve better metal removal rate, surface finish and cutting width simultaneously.

Keywords WEDM · Metal removal rate · Surface finish · Kerf · Taguchi method · Genetic algorithm

S. S. Mahapatra (✉)
Department of Mechanical Engineering,
National Institute of Technology,
Rourkela, India
e-mail: mahapatras2003@yahoo.com

A. Patnaik
Department of Mechanical Engineering,
Gandhi Institute of Engineering & Technology,
Gunupur, India

1 Introduction

In recent years, the technology of wire electrical discharge machining (WEDM) has been improved significantly to meet the requirements in various manufacturing fields, especially in the precision die industry. WEDM is a thermo-electrical process in which material is eroded from the workpiece by a series of discrete sparks between the workpiece and the wire electrode (tool) separated by a thin film of dielectric fluid (deionized water) that is continuously fed to the machining zone to flush away the eroded particles. The movement of wire is controlled numerically to achieve the desired three-dimensional shape and accuracy of the workpiece. The schematic diagram of WEDM is shown in Fig. 1 along with dielectric flow, power supply, working table and other control devices. It is evident from Fig. 1 that it is absolutely essential to hold the wire in a designed position against the object because the wire repeats complex oscillations due to electro-discharge between the wire and workpiece. Normally, the wire is held by a pin guide at the upper and lower parts of the workpiece. In most cases, the wire will be discarded once used. However, there are problematic points that should be fully considered in order to enhance working accuracy. According to Trezise [1], the fundamental limits on machining accuracy are dimensional consistency of the wire and the positional accuracy of the worktable. Most of the uncertainties arise because the working region is an unsupported section of the wire, remote from the guides. The detailed section of the working region of the wire electrode is shown in Fig. 2.

Rajurkar and Wang [2] analyzed the wire rupture phenomena with a thermal model. An extensive experimental investigation has been carried out to determine the variation of machining performance outputs viz., MRR and

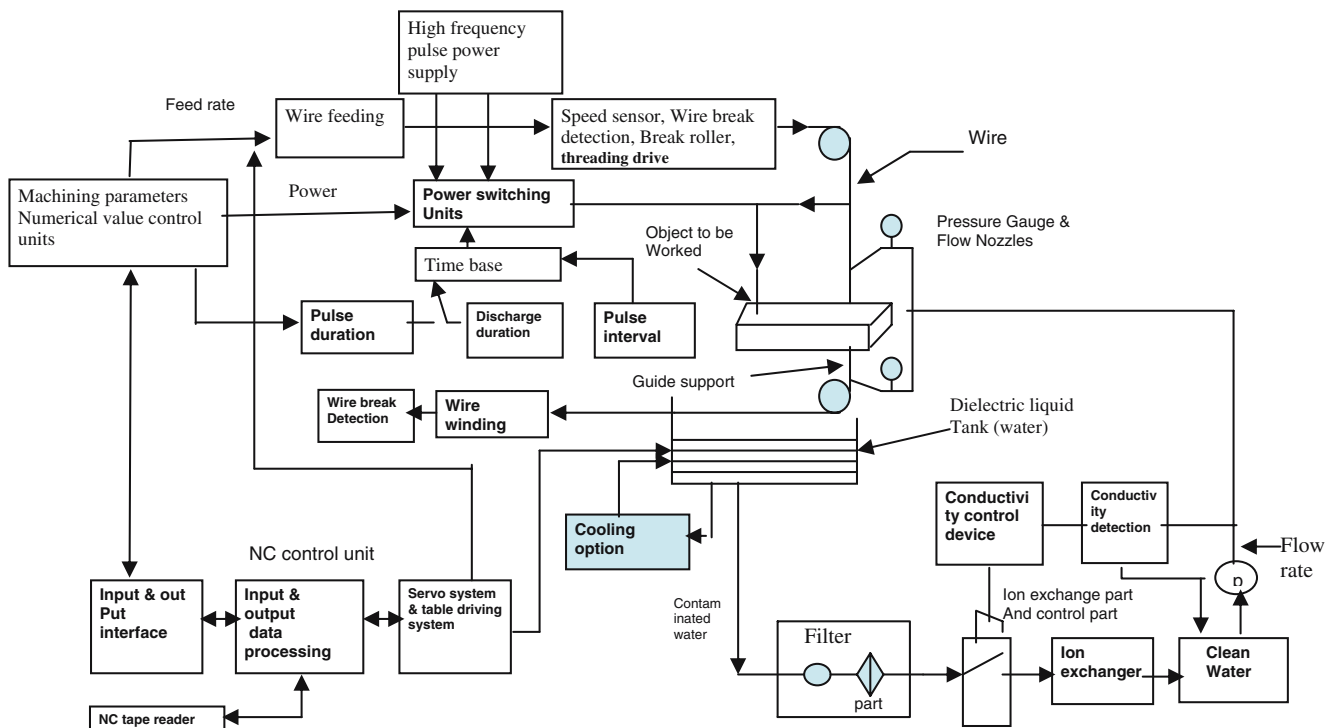


Fig. 1 Schematic diagram of WEDM

SF with machining parameters in the study. Targ et al. [3] used a neural network system to determine settings of pulse duration, pulse interval, peak current, open circuit voltage, servo reference voltage, electric capacitance, and table speed for the estimation of cutting speed and surface finish. Scott et al. [4] used a factorial design method to determine the optimal combination of control parameters in WEDM, the measures of machining performance being the metal removal rate and the surface finish. Based on the analysis of variance, it was found that the discharge current, pulse

duration, and pulse frequency are significant control factors for both the metal removal rate and surface roughness. Lok and Lee [5] compared the machining performance in terms of MRR and surface finish through observations obtained by processing of two advanced ceramics under different cutting conditions using WEDM. Huang et al. [6] investigated experimentally the effect of machining parameters on the gap width, the surface roughness, and the depth of white layer on the machined workpiece surface. Rozenek et al. [7] used a metal matrix composite as workpiece material

Fig. 2 Detail of WEDM cutting gap

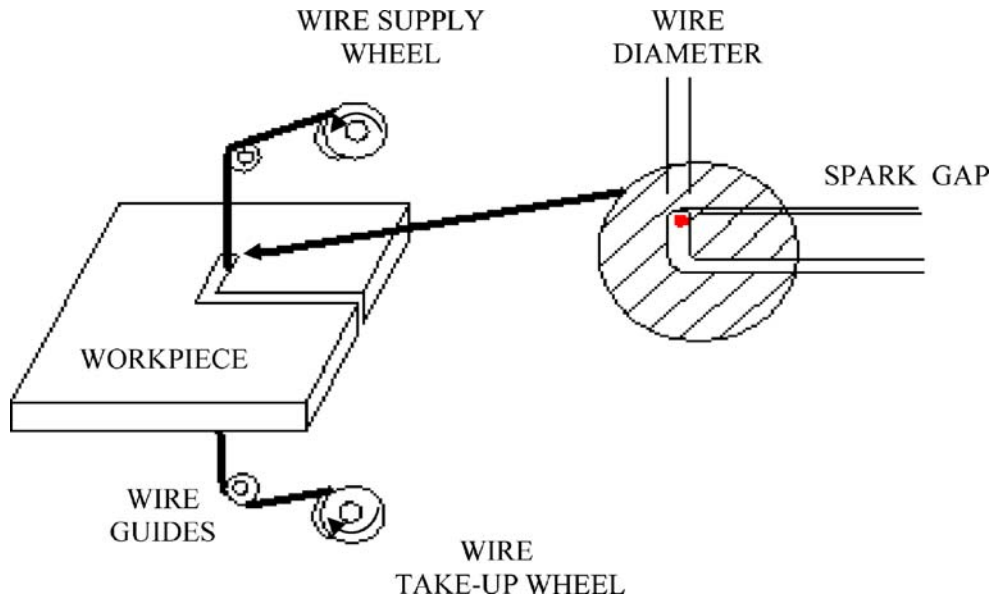
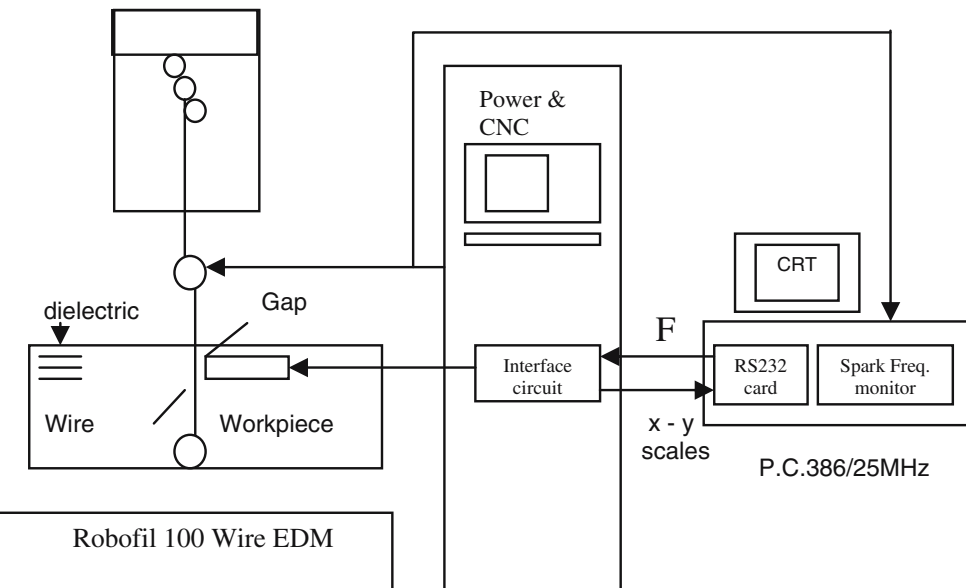


Fig. 3 Experimental set-up of Robofil100 WEDM



and investigated the variation of machining feed rate and surface roughness with machining parameters. Tosun and Cogun [8] investigated the effect of machining parameters on wire wear ratio based on the weight loss of wire in WEDM. Tosun et al. [9] introduced a statistical approach to determine the optimal machining parameters for minimum size of wire craters in WEDM.

The most important performance measures in WEDM are metal removal rate, surface finish, and cutting width (kerf). They depend on machining parameters like discharge current, pulse duration, pulse frequency, wire speed, wire tension and dielectric flow rate. Among other performance measures, the kerf, which determines the dimensional accuracy of the finishing part, is of extreme importance. The internal corner radius to be produced in WEDM operations is also limited by the kerf. The gap between the wire and workpiece usually ranges from 0.025 to 0.075 mm and is constantly maintained by a computer controlled positioning system. In WEDM operations, material removal rate determines the economics of machining and rate of production where as kerf denotes degree of precision.

In setting the machining parameters, particularly in rough cutting operation, the goal is three fold: the maximization of MRR, maximization of SF, and minimization of kerf. Generally, the machine tool builder provides machining parameter table to be used for setting machining parameter. This process relies heavily on the experience of the operators. In practice, it makes very difficult to utilize the optimal functions of a machine owing to there being too many adjustable machining parameters. With a view to alleviate this difficulty, a simple but reliable method based on statistically designed experiments is suggested for investigating the effects of various process parameters on MRR, SF and kerf and determines optimal process settings. The Taguchi method, a powerful experimental design tool, uses simple, effective, and systematic approach for deriving of the optimal machining parameters. Further, this approach requires minimum experimental cost and efficiently reduces the effect of the source of variation. An inexpensive and easy-to-operate methodology must be evolved to modify the machined surfaces as well as maintain accuracy. The methodology uses Taguchi's experimental design for setting suitable machining parameters in order to effectively

Table 1 Parameters of the setting

Control factors	Symbols	Fixed parameters	
Discharge current	Factor A	Wire	Zinc-coated copper wire
Pulse duration	Factor B	Shape	Rectangular product
Pulse frequency	Factor C	Location of work piece on working table	At the center of the table
Wire speed	Factor D	Angle of cut	Vertical
Wire tension	Factor E	Thickness of work piece	10 mm
Dielectric flow rate	Factor F	Stability	Servo control
		Height of work piece	25 mm
		Wire type	Stratified, copper, diameter 0.25 mm

Table 2 Levels for various control factors

Control factor	I	II	III	Unit
A. Discharge current	16.00	24.00	32.00	Amp
B. Pulse duration	3.20	6.40	12.80	μs
C. Pulse frequency	40.00	50.00	60.00	KHz
D. Wire speed	7.60	8.60	9.20	m/min
E. Wire tension	1,000.00	1,100.00	1,200.00	g
F. Dielectric flow rate	1.20	1.30	1.40	Bars

control the amount of removed materials and to produce complicated precise components.

2 Experimental method

The experiments were performed on ROBOFIL 100 high-precision 5 axis CNC WEDM, which is manufactured by Charmilles Technologies Corporation. The basic parts of the WEDM machine consists of a wire, a worktable, a servo control system, a power supply and dielectric supply system. The ROBOFIL 100 allows the operator to choose input parameters according to the material and height of the workpiece and tool material from a manual provided by the WEDM manufacturer. The ROBOFIL 100 WED machine has several special features. The pulse power supply uses a transistor controlled RC circuit. The discharge energy is determined by the value of the capacitor that is parallel to the machining gap. The experimental set-up for the data acquisition of the sparking frequency and machine table speed is illustrated in Fig. 3.

2.1 Material, test conditions and measurement

The input and fixed parameters used in the present study are also listed in Table 1. These were chosen through review of literature, experience, and some preliminary investigations. Different settings of discharge current, pulse duration, pulse frequency, wire speeds, wire tension, and dielectric flow rate used in the experiments are shown in Table 2. Each time an experiment was performed, a particular set of input parameters was chosen and the workpiece, a block of D2 tool steel (1.5% C, 12% Cr, 0.6% V,

1% Mo, 0.6% Si, 0.6% Mn and balance Fe) with $200 \times 25 \times 10$ mm size, was cut 100 mm in length with 10 mm depth along the longer length. A 0.25-mm diameter stratified wire (zinc coated copper wire) with vertical configuration was used and discarded once used. High MRR in WEDM without wire breakage can be attained by the use of a zinc-coated copper wire because evaporation of zinc causes cooling at the interface of workpiece and wire and a coating of zinc oxide on the surface of the wire helps prevent short-circuits [10].

The most important performance measures in WEDM are metal removal rate, workpiece surface finish and cutting width. The surface finish value (in μm) was obtained by measuring the mean absolute deviation, R_a (surface roughness) from the average surface level using a type C3A Mahr Perthen Perthometer (stylus radius of 5 μm). The kerf was measured using the Mitutoyo tools makers' microscope (x100), is expressed as sum of the wire diameter and twice of wire-workpiece gap. The kerf value is the average of five measurements made from the workpiece with 20-mm increments along the cut length. MRR is calculated as,

$$MRR = k \cdot t \cdot v_c \cdot \rho \quad (1)$$

Here, k is the kerf, t is the thickness of workpiece (10 mm), v_c is cutting speed and ρ is the density of the workpiece material (7.8 g/cm^3).

2.2 Design of experiment based on Taguchi method

The WEDM process consists of three operations, a roughing operation, a finishing operation, and a surface finishing operation. Usually, performance of various types of cutting operations is judged by different measures. In case of finish cutting operation, the surface finish is of primary importance whereas both metal removal rate and surface finish are of primary importance for rough cutting operation. Dimensional accuracy is highly dependent on cutting width. This means that the rough cutting operation is more challenging because three goals must be satisfied simultaneously. Therefore, the rough cutting phase is investigated

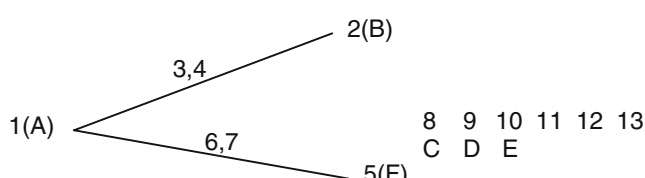
**Fig. 4** Modified linear graph for L_{27}

Table 3 Orthogonal array for L₂₇(3¹³) Taguchi design

L ₂₇ (3 ¹³)	1 A	2 B	3 (Ax B) ₁	4 (Ax B) ₂	5 F	6 (Ax F) ₁	7 (Ax F) ₁	8 C	9 D	10 E	11	12	13
1	1	1	1	1	1	1	1	1	1	1	1	1	1
2	1	1	1	1	2	2	2	2	2	2	2	2	2
3	1	1	1	1	3	3	3	3	3	3	3	3	3
4	1	2	2	2	1	1	1	2	2	2	3	3	3
5	1	2	2	2	2	2	2	3	3	3	1	1	1
6	1	2	2	2	3	3	3	1	1	1	2	2	2
7	1	3	3	3	1	1	1	3	3	3	2	2	2
8	1	3	3	3	2	2	2	1	1	1	3	3	3
9	1	3	3	3	3	3	3	2	2	2	1	1	1
10	2	1	2	3	1	2	3	1	2	3	1	2	3
11	2	1	2	3	2	3	1	2	3	1	2	3	1
12	2	1	2	3	3	1	2	3	1	2	3	1	2
13	2	2	3	1	1	2	3	2	3	1	3	1	2
14	2	2	3	1	2	3	1	3	1	2	1	2	3
15	2	2	3	1	3	1	2	1	2	3	2	3	1
16	2	3	1	2	1	2	3	3	1	2	2	3	1
17	2	3	1	2	2	3	1	1	2	3	3	1	2
18	2	3	1	2	3	1	2	2	3	1	1	2	3
19	3	1	3	2	1	3	2	1	3	2	1	3	2
20	3	1	3	2	2	1	3	2	1	3	2	1	3
21	3	1	3	2	3	2	1	3	2	1	3	2	1
22	3	2	1	3	1	3	2	2	1	3	3	2	1
23	3	2	1	3	2	1	3	3	2	1	1	3	2
24	3	2	1	3	3	2	1	1	3	2	2	1	3
25	3	3	2	1	1	3	2	3	2	1	2	1	3
26	3	3	2	1	2	1	3	1	3	2	3	2	1
27	3	3	2	1	3	2	1	2	1	3	1	3	2

in the present approach considering three performance goals like MRR, SF, and kerf. The experiment is carried out on the ROBOFIL 100 WEDM, the input parameters to be chosen from a limited set of possible values. The values of input parameters, which are of interest in the rough cut with finishing phase, are recorded. To evaluate the effects of machining parameters on performance characteristics (MRR, SF, and kerf) and to identify the performance characteristics under the optimal machining parameters, a special designed experimental procedure is required. In this study, the Taguchi method, a powerful tool for parameter design of the performance characteristics was used to determine optimal machining parameters for maximization of MRR, SF, and minimization of kerf in WEDM. The control factors are used to select the best conditions for stability in design of manufacturing process, whereas the noise factors denote all factors that cause variation. In this work, it is planned to study the behavior of six control factors viz., A, B, C, D, E, and F and two interactions viz., A×B and A×F based on past experience. The experimental observations are further transformed into a signal-to-noise (S/N) ratio. There are several S/N ratios available depending on the type of characteristics. The characteristic that

higher value represents better machining performance, such as MRR, is called ‘higher is better, HB’. Inversely, the characteristic that lower value represents better machining performance, such as surface roughness, is called ‘lower is better, LB’. Therefore, “HB” for the MRR ’LB’ for the SF and “LB” for the kerf were selected for obtaining optimum machining performance characteristics were selected for obtaining optimum machining performance characteristics. The loss function (L) for objective of HB and LB is defined as follows:

$$L_{HB} = \frac{1}{n} \sum_{i=1}^n \frac{1}{y_{MRR}^2} \quad (2)$$

$$L_{LB} = \frac{1}{n} \sum_{i=1}^n y_{SF}^2 \quad (3)$$

$$L_{LB} = \frac{1}{n} \sum_{i=1}^n y_{kerf}^2 \quad (4)$$

Table 4 Experimental design using L₂₇ orthogonal array

Expt. no.	A	B	F	C	D	E	MRR (g/min)	S/N ratio (db)	R _a (μm)	S/N ratio (db)	Kerf (mm)	S/N ratio (db)
1	1	1	1	1	1	1	0.139939	-17.0812	3.68	88.6820	0.236	12.5418
2	1	1	2	2	2	2	0.127569	-17.8851	3.61	88.8514	0.190	14.4249
3	1	1	3	3	2	3	0.115264	-18.7661	3.53	89.0493	0.161	15.8635
4	1	2	1	2	2	2	0.169761	-15.4032	3.82	88.3584	0.286	10.8727
5	1	2	2	3	3	3	0.150028	-16.4766	3.77	88.4805	0.224	12.9950
6	1	2	3	1	1	1	0.156325	-16.1195	3.70	88.6461	0.217	13.2708
7	1	3	1	3	3	3	0.182900	-14.7557	3.86	88.2607	0.308	10.2290
8	1	3	2	1	1	1	0.166973	-15.5471	3.83	88.3468	0.248	12.1110
9	1	3	3	2	2	2	0.146937	-16.6574	3.77	88.4688	0.204	13.8074
10	2	1	1	1	2	3	0.141560	-16.9812	3.64	88.7723	0.211	13.5144
11	2	1	2	2	3	1	0.132273	-17.5706	3.63	88.8088	0.184	14.7036
12	2	1	3	3	1	2	0.151855	-16.3714	3.67	88.7120	0.256	11.8352
13	2	2	1	2	3	1	0.222566	-13.0508	3.89	88.1925	0.332	9.5772
14	2	2	2	3	1	2	0.219497	-13.1714	3.87	88.2436	0.306	10.2856
15	2	2	3	1	2	3	0.220792	-13.1203	3.90	88.1698	0.372	8.5891
16	2	3	1	3	1	2	0.165344	-15.6322	3.86	88.2722	0.246	12.1813
17	2	3	2	1	2	3	0.156703	-16.0985	3.83	88.3295	0.218	13.2309
18	2	3	3	2	3	1	0.165329	-15.6330	3.86	88.2722	0.278	11.1191
19	3	1	1	1	3	2	0.168143	-15.4864	3.73	88.5755	0.234	12.6157
20	3	1	2	2	1	3	0.174135	-15.1823	3.75	88.5098	0.294	10.6331
21	3	1	3	3	2	1	0.170947	-15.3428	3.73	88.5688	0.254	11.9033
22	3	2	1	2	1	3	0.161285	-15.8481	3.80	88.4047	0.225	12.9563
23	3	2	2	3	2	1	0.169096	-15.4373	3.84	88.3123	0.285	10.9031
24	3	2	3	1	3	2	0.169818	-15.4004	3.83	88.3353	0.253	11.9376
25	3	3	1	3	2	1	0.188897	-14.4755	3.99	88.9833	0.263	11.6009
26	3	3	2	1	3	2	0.155701	-16.1542	3.89	88.2038	0.262	11.6340
27	3	3	3	2	1	3	0.174034	-15.1873	3.89	88.1982	0.259	11.7340

where y_{MRR} , y_{SF} and y_{kerf} response for metal removal rate, surface finish and cutting width, respectively, and n denotes the number of experiments.

The S/N ratio can be calculated as a logarithmic transformation of the loss function as shown below.

$$\text{S/N ratio for MRR} = -10 \log_{10} (L_{HB}) \quad (5)$$

$$\text{S/N ratio for SF} = -10 \log_{10} (L_{LB}) \quad (6)$$

$$\text{S/N ratio for kerf} = -10 \log_{10} (L_{LB}) \quad (7)$$

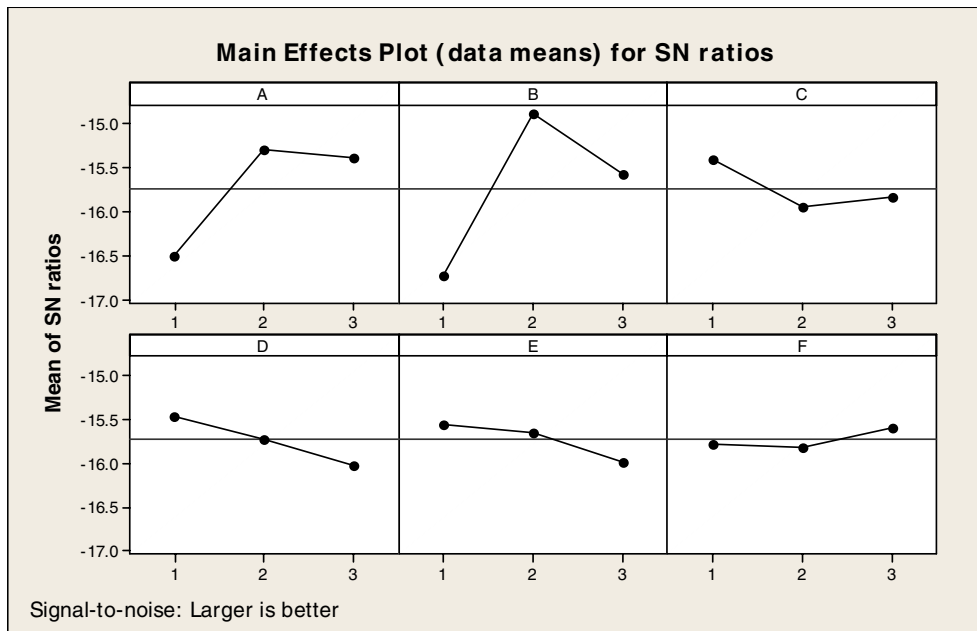
The standard linear graph is modified using the line separation method, as shown in Fig. 4, to assign the factors and interactions to various columns of the orthogonal array [11, 12]. The array chosen was the L₂₇ (3¹³), which has 27 rows corresponding to the number of experiments with 13 columns at three levels, as shown in Table 3. The factors and their interaction are assigned to the columns by modifying the standard linear graph. The plan of experiments is as follows: the first column was assigned to discharge current (A), the second column to pulse duration (B), the fifth column to dielectric flow rate (F), the eighth column to pulse frequency (C), ninth column to wire speed

(D), the tenth column to wire tension (E), the third column and fourth column are assigned to (A×B)₁ and (A×B)₂, respectively, to estimate interaction between discharge current (A) and pulse duration (B), the sixth column and the seventh column are assigned to (A×F)₁ and (A×F)₂, respectively, to estimate interaction between the discharge current (A) and dielectric flow rate (F). According to the Taguchi design concept, a L₂₇ orthogonal array table was chosen for the experiments is shown in Table 4. The experiments were conducted for each combination of factors (rows) as per selected orthogonal array (Fig. 4). The number of observation under each combination of factors is one i.e., the number of replications is one.

3 Result and discussion

From Table 4, the overall mean for the S/N ratio of MRR, SF and kerf is found to be -15.04 db, 88.78 db, and 12.11 db, respectively. Figures 5, 6 and 7 show graphically the effect of the six control factors on MRR, SF and kerf, respectively. The analysis was made using the popular software specifically used for design of experiment applications known as MINITAB 14. Before any attempt is

Fig. 5 Effect of control factors on MRR



made to use this simple model as a predictor for the measures of performance, the possible of interactions between the factors must be considered. Thus factorial design incorporates a simple means of testing for the presence of the interaction effects. The S/N ratio response table and response graphs are shown for S/N ratio for MRR in Table 5 and Fig. 5, respectively. Similarly, response table and response graphs are shown for S/N ratio for SF in Table 6 and Fig. 6, respectively. The response table and

associated response graph for kerf are shown in Table 7 and Fig. 7, respectively. Analysis of the result leads to the conclusion that factors at level A₂, B₂, C₁, D₁, E₁ and F₃ gives maximum MRR. Although factors A, B, and F do not show significant effect but significant interaction between factors A and B and A and F is observed for material removal rate as shown in Figs. 8 and 9. Factor F is having least significance effect for improving MRR. Similarly, it is recommended to use the factors at level A₁, B₁, C₁, D₃, E₃

Fig. 6 Effect of control factors on SF

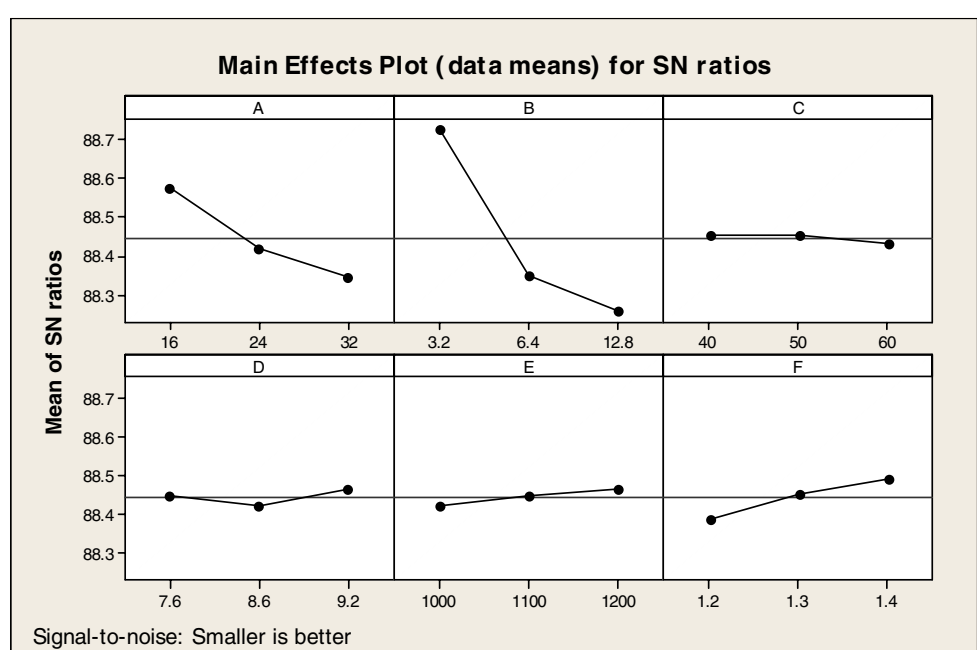
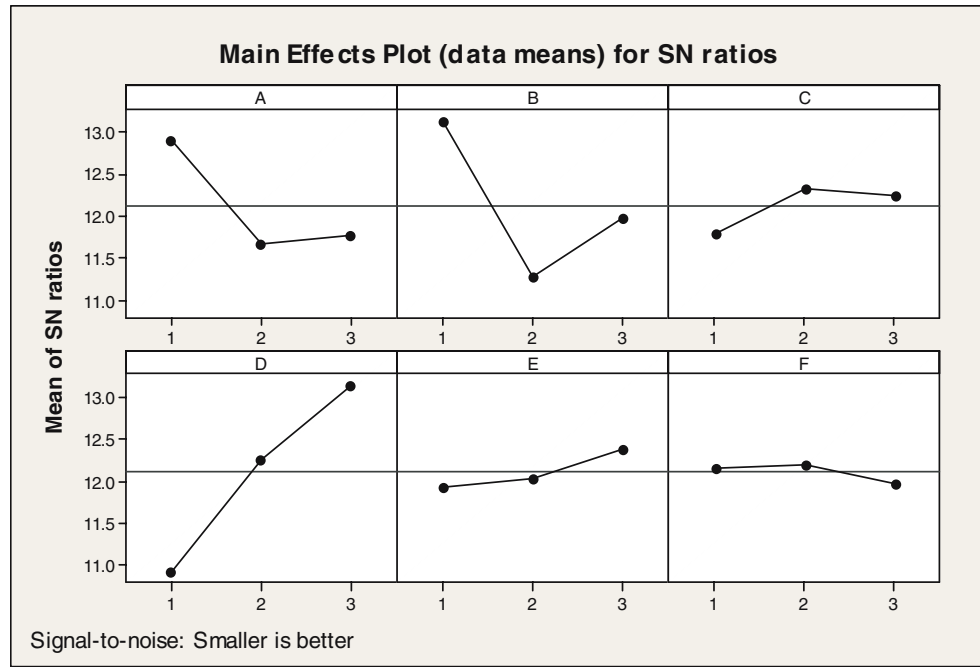


Fig. 7 Effect of control factors on kerf



and F_3 for maximization of SF and the interaction graphs are shown in Figs. 10 and 11. Factors C, D, and E have least contribution for maximization of SF. However, interaction between factors A and B and A and F cannot be neglected. The factor combination for minimization of kerf is given as A_1, B_1, C_2, D_3, E_3 and F_2 and interaction curves are shown in Figs. 12 and 13. As far as kerf is concerned, factor D is the most important factor among all factors whereas factor F has least effect. The effect of factors C, E and F seems to be less significant but interaction between factors A and B and A and F cannot be neglected. It is interesting to note that optimal settings of parameters for MRR, SF and kerf are quite different and poses difficulty to achieve the goals of all objectives.

4 Confirmation experiment

The optimal combination of machining parameters has been determined in the previous analysis. However, the final step is to predict and verify the improvement of the observed values through the use of the optimal combination level of

machining parameters. The estimated S/N ratio for MRR can be calculated with the help of following prediction equation:

$$\begin{aligned} \hat{\eta}_1 = & \bar{T} + (\bar{A}_2 - \bar{T}) + (\bar{B}_3 - \bar{T}) \\ & + [(\bar{A}_2 \bar{B}_3 - \bar{T}) - (\bar{A}_2 - \bar{T}) - (\bar{B}_3 - \bar{T})] \\ & + (\bar{F}_2 - \bar{T}) + [(\bar{A}_2 \bar{F}_2 - \bar{T}) - (\bar{A}_2 - \bar{T}) - (\bar{F}_2 - \bar{T})] \\ & + (\bar{C}_2 - \bar{T}) + (\bar{D}_3 - \bar{T}) + (\bar{E}_1 - \bar{T}) \end{aligned} \quad (8)$$

$\frac{\hat{\eta}_1}{\bar{T}}$ Predicted Average
 $\bar{A}_2, \bar{B}_3, \bar{F}_2, \bar{C}_2, \bar{D}_3$, and \bar{E}_1 Overall experimental average
 Mean response for factors and interactions at designated levels.

By combining like terms, the equation reduces to

$$\hat{\eta}_1 = \bar{A}_2 \bar{B}_3 - \bar{A}_2 + \bar{A}_2 \bar{F}_2 + \bar{C}_2 + \bar{D}_3 + \bar{E}_1 - 3\bar{T} \quad (9)$$

A new combination of factor levels $A_2 B_3 C_2 D_3 E_1 F_2$ is used to predict MRR through prediction equation and it is found to be $\bar{\eta}_1 = -16.4515db$.

Table 5 S/N ratio response table for MRR

	A	B	AXB_1	AXB_2	F	AXF_1	AXF_2	C	D	E
Level 1	-16.52	-16.74	-16.42	-15.43	-15.78	-15.46	-15.56	-15.41	-15.46	-15.56
Level 2	-15.29	-14.89	-16.08	-15.71	-15.82	-15.72	-15.65	-15.95	-15.72	-15.65
Level 3	-15.39	-15.57	-14.70	-16.06	-15.60	-16.02	-15.99	-15.84	-16.02	-16.00
Delta	1.23	1.85	1.72	0.63	0.22	0.56	0.43	0.53	0.56	0.44

Table 6 S/N ratio response table for SF

	A	B	(AXB) ₁	(AXB) ₂	F	(AXF) ₁	(AXF) ₂	C	D	E
Level 1	88.57	88.72	88.50	88.40	88.39	88.39	88.42	88.45	88.44	88.42
Level 2	88.42	88.35	88.46	88.44	88.45	88.45	88.42	88.45	88.43	88.45
Level 3	89.34	89.26	88.37	89.49	88.49	88.50	88.49	88.43	88.46	88.47
Delta	0.23	0.46	0.13	0.09	0.10	0.11	0.07	0.02	0.04	0.05

Similarly, a prediction equation is developed for estimating S/N ratio of SF as given in Eq. (10).

$$\begin{aligned} \hat{\eta}_2 = & \bar{T} + (\bar{A}_3 - \bar{T}) + (\bar{B}_2 - \bar{T}) \\ & + [(\bar{A}_3\bar{B}_2 - \bar{T}) - (\bar{A}_3 - \bar{T}) - (\bar{B}_2 - \bar{T})] + (\bar{F}_1 - \bar{T}) \\ & + [(\bar{A}_3\bar{F}_1 - \bar{T}) - (\bar{A}_3 - \bar{T}) - (\bar{F}_1 - \bar{T})] \\ & + (\bar{C}_3 - \bar{T}) + (\bar{D}_2 - \bar{T}) + (\bar{E}_2 - \bar{T}) \end{aligned} \quad (10)$$

$\frac{\hat{\eta}_2}{\bar{T}}$ Predicted Average
 $\bar{A}_3, \bar{B}_2, \bar{F}_1, \bar{C}_3, \bar{D}_2$, and \bar{E}_2 Overall experimental average
 $\bar{A}_3, \bar{B}_2, \bar{F}_1, \bar{C}_3, \bar{D}_2$, and \bar{E}_2 Mean response for factors and interactions at designated levels.

Again by combining like terms, the equation reduces to

$$\hat{\eta}_2 = \bar{A}_3\bar{B}_2 - \bar{A}_3 + \bar{A}_3\bar{F}_1 + \bar{C}_3 + \bar{D}_2 + \bar{E}_2 - 3\bar{T} \quad (11)$$

A new experimental set up with factor levels at A₃ B₂ C₃ D₂ E₂ F₁ is considered to predict the S/N ratio for SF and is found to be $\hat{\eta}_2 = 86.75db$.

Similarly, a prediction equation is developed for estimating S/N ratio of kerf as given in Eq. (12).

$$\begin{aligned} \hat{\eta}_3 = & \bar{T} + (\bar{A}_1 - \bar{T}) + (\bar{B}_2 - \bar{T}) \\ & + [(\bar{A}_1\bar{B}_2 - \bar{T}) - (\bar{A}_1 - \bar{T}) - (\bar{B}_2 - \bar{T})] + (\bar{F}_1 - \bar{T}) \\ & + [(\bar{A}_1\bar{F}_1 - \bar{T}) - (\bar{A}_1 - \bar{T}) - (\bar{F}_1 - \bar{T})] \\ & + (\bar{C}_1 - \bar{T}) + (\bar{D}_2 - \bar{T}) + (\bar{E}_3 - \bar{T}) \end{aligned} \quad (12)$$

$\frac{\hat{\eta}_3}{\bar{T}}$ Predicted Average
 $\bar{A}_1, \bar{B}_2, \bar{F}_1, \bar{C}_1, \bar{D}_2$, and \bar{E}_3 Overall experimental average
 $\bar{A}_1, \bar{B}_2, \bar{F}_1, \bar{C}_1, \bar{D}_2$, and \bar{E}_3 Mean response for factors and interactions at designated levels.

By combining like terms, the equation reduces to

$$\hat{\eta}_3 = \bar{A}_1\bar{B}_2 - \bar{A}_1 + \bar{A}_1\bar{F}_1 + \bar{C}_1 + \bar{D}_2 + \bar{E}_3 - 3\bar{T} \quad (13)$$

A new experimental set up with factor levels at A₁B₂ C₁D₂E₃F₁ is considered to predict the S/N ratio for kerf and is found to be $\hat{\eta}_3 = 10.7540db$.

For each performance measure, an experiment was conducted for a different factor combination and compared with the result obtained from the predictive equation as shown in Tables 8, 9 and 10. The resulting model seems to be capable of predicting MRR, SF and kerf to a reasonable accuracy. An error of 3.14% for the S/N ratio of MRR, 1.95% for the S/N ratio of SF and 3.72% for the S/N ratio of kerf is observed. However, the errors can be further reduced if the number of measurements is increased. This validates the development of the mathematical model for predicting the measures of performance based on knowledge of the input parameters.

5 Multi-objective optimization of WEDM parameters

Machining settings that satisfy multiple objectives of maximization of MRR and SF and minimization of kerf need to be determined. The mathematical model suggested here is in the following form.

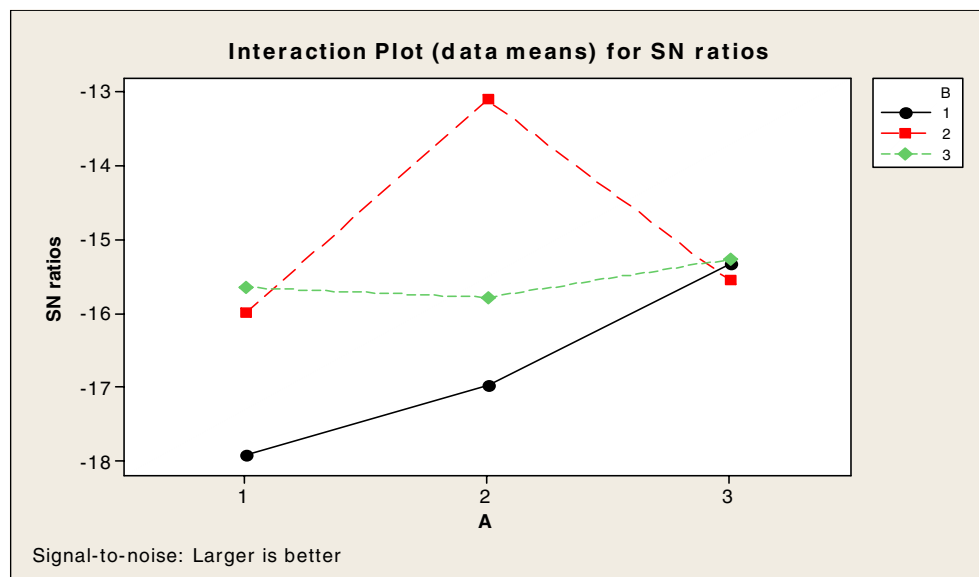
$$\begin{aligned} Y = & K_0 + K_1 \times A + K_2 \times B + K_3 \times C + K_4 \times D \\ & + K_5 \times E + K_6 \times F + K_7 \times A \times B + K_8 \times A \\ & \times F \end{aligned} \quad (14)$$

Here, Y is the performance output terms and K_i (i=0, ..., 8) are the model constants. The constants were calculated by using non-linear regression analysis method with the help of MINITAB 14 software. The calculated

Table 7 S/N ratio response table for kerf

	A	B	AXB ₁	AXB ₂	F	AXF ₁	AXF ₂	C	D	E
Level 1	12.90	13.12	13.12	11.80	12.16	10.93	11.94	11.79	10.93	11.94
Level 2	11.67	11.27	11.26	12.09	12.20	12.26	12.03	12.32	12.26	12.03
Level 3	11.77	11.96	11.96	12.44	11.98	13.15	11.38	12.23	13.15	12.34
Delta	1.23	1.85	1.86	0.64	0.23	2.22	0.65	0.54	2.22	0.44

Fig. 8 Interaction graph between A×B for MRR



coefficients from MINITAB software were substituted in Eq. (14) and following relations were obtained.

$$\begin{aligned} MRR = & 0.427 + 0.477A + 0.380B - 0.052C \\ & - 0.061D + 0.106E - 0.032F - 0.366AB \\ & - 0.152AF \end{aligned} \quad (15)$$

$$r^2 = 0.98$$

$$\begin{aligned} SF = & 0.894 + 0.540A + 0.095B - 0.12C - 0.004D \\ & + 0.106E - 0.106F - 0.031AB - 0.003AF \end{aligned} \quad (16)$$

$$r^2 = 0.98$$

$$\begin{aligned} Kerf = & 0.373 + 0.433A + 0.349B - 0.039C \\ & - 0.045D + 0.106E - 0.028F - 0.366AB \\ & - 0.152AF \end{aligned} \quad (17)$$

$$r^2 = 0.97$$

Fig. 9 Interaction graph between A×F for MRR

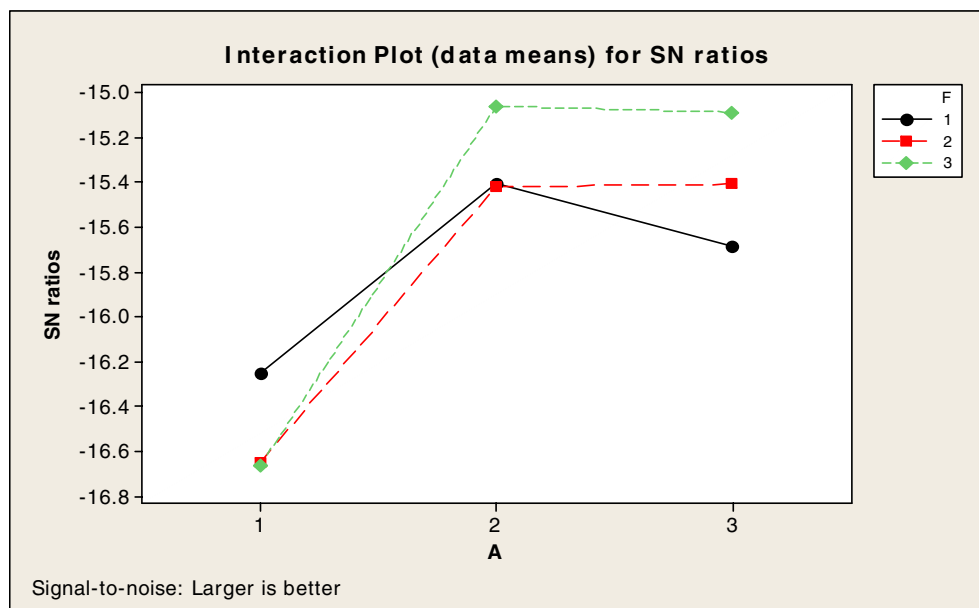
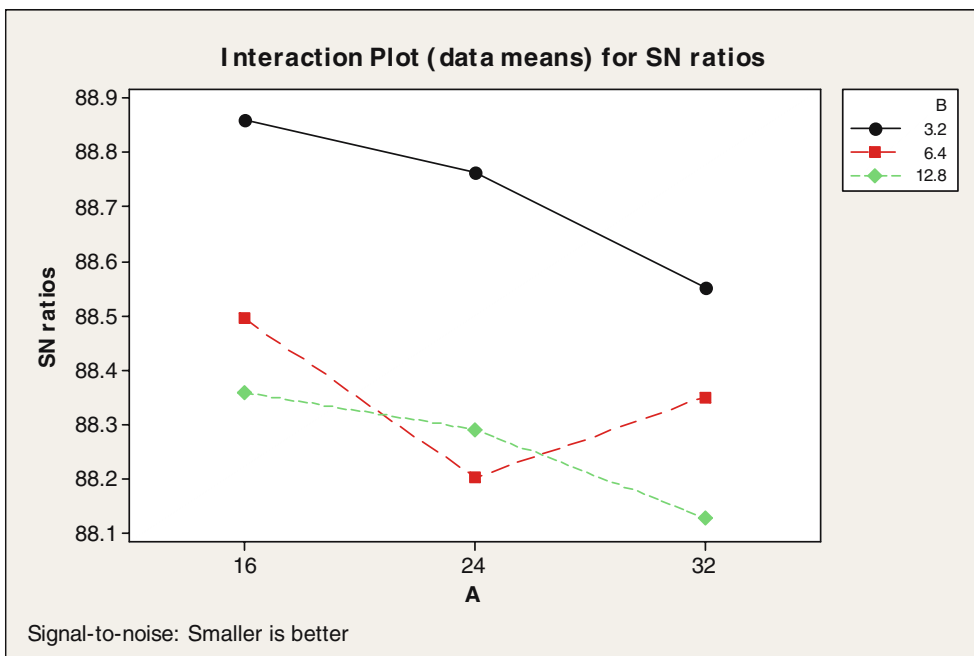


Fig. 10 Interaction graph between A×B for SF



The higher correlation coefficients (r^2) confirm the suitability of the used model and the correctness of the calculated constants. In this study, a weighting method is used for the optimization of the process with multi-machining performance outputs. Since the MRR, SF, and kerf are the three different objects, in order to overcome the large differences in numerical values between the objects, the function corresponds to every

machining performance output is normalized first. A weighting method is adopted to the normalize the performance output, such as MRR, SF and kerf to a single object. Here, the resultant weighted objective function to be maximized is:

$$\text{Maximize } Z = (w_1 \times f_1 + w_2 \times 1/f_2 + w_3 \times 1/f_3)(1 - K.C) \quad (18)$$

Fig. 11 Interaction graph between A×F for SF

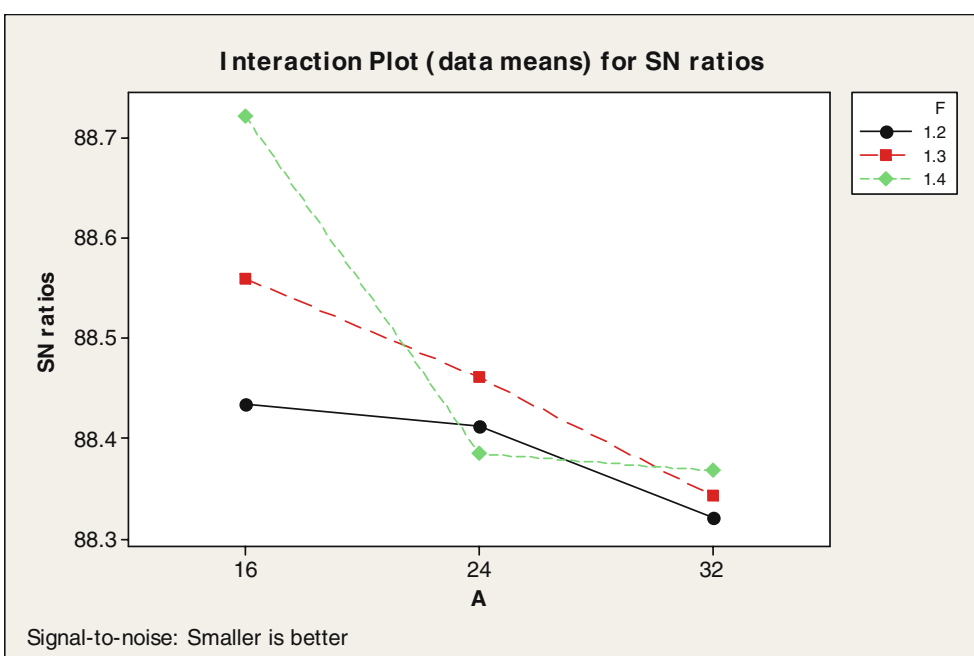
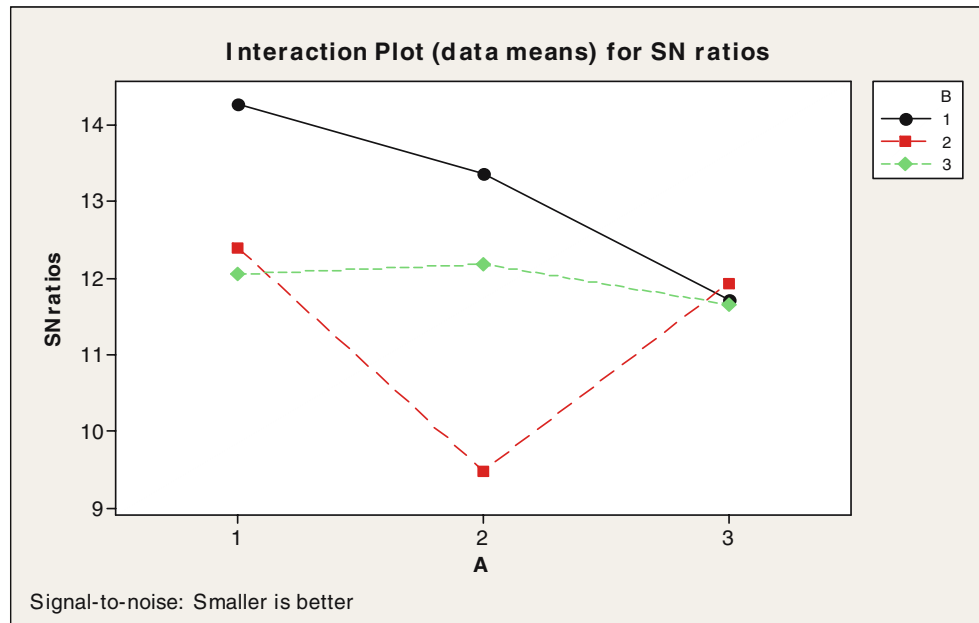


Fig. 12 Interaction graph between A×B for kerf



f_1 Normalized function for MRR

$$C_{min} \leq C \leq C_{max} \quad (21)$$

f_2 Normalized function for SF

f_3 Normalized function for kerf

$$D_{min} \leq D \leq D_{max} \quad (22)$$

C violation coefficient

K a penalty parameter, usually the value is 10

Subjected to constraints:

$$E_{min} \leq E \leq E_{max} \quad (23)$$

$$A_{min} \leq A \leq A_{max} \quad (19)$$

$$F_{min} \leq F \leq F_{max} \quad (24)$$

$$B_{min} \leq B \leq B_{max} \quad (20)$$

Fig. 13 Interaction graph between A×F for kerf

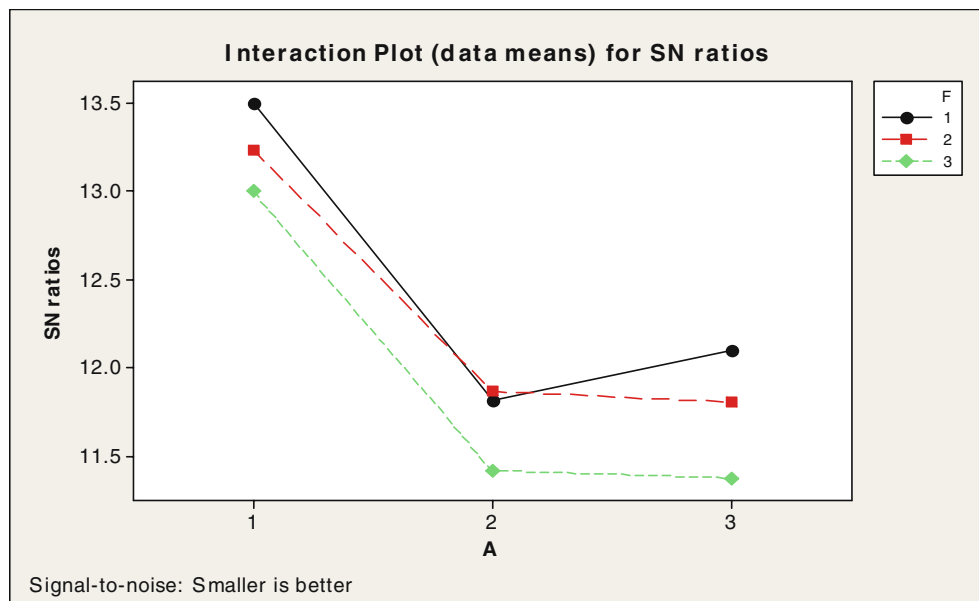


Table 8 Results of the confirmation experiment for MRR

	Optimal machining parameter	
	Prediction	Experimental
Level	A ₂ B ₃ F ₂ C ₂ D ₃ E ₁	A ₂ B ₃ F ₂ C ₂ D ₃ E ₁
S/N ratio for MRR (db)	-16.4515	-16.9854

where w_1 , w_2 and w_3 are the weighting factors of the for normalized MRR, SF and kerf functions used in the objective function of optimization process. The weighting factors are selected in such a manner that their sum is equal to one. A higher weighting factor for an objective indicates more emphasis on it. The min and max in Eqs. (19), (20), (21), (22), (23), (24) represent lowest and highest control factor settings, respectively, (Table 2).

Genetic algorithm (GA) was used to obtain the optimum machining parameters for multi-objective outputs by using the several combinations of the weight. The larger the weighting factor, the greater the improvement in the machining performance outputs. To optimize the multi-objective function, the GA parameters are summarized in Table 11. The computational algorithm was implemented in C++ code. Genetic algorithms (GAs) are mathematical optimization techniques that simulate a natural evolution process. They are based on the Darwinian Theory, in which the fittest species survives and propagates while the less successful tend to disappear. The concept of genetic algorithm is based on the evolution process and was introduced by Holland [13]. Genetic algorithm mainly depends on the following types of operators: reproduction, crossover, and mutation. Reproduction is accomplished by copying the best individuals from one generation to the next, in what is often called an elistic strategy. The best solution is monotonically improving from one generation to the next. The selected parents are submitted to the crossover operator to produce one or two children. The crossover is carried out with an assigned probability, which is generally rather high. If a number randomly sampled is inferior to the probability, the crossover is performed. The genetic mutation introduces diversity in the population by an occasional random replacement of the individuals. The mutation is performed based on an assigned probability. A random number is used to determine if a new individual

Table 10 Results of the confirmation experiment for kerf

	Optimal machining parameter	
	Prediction	Experimental
Level	A ₁ B ₂ F ₁ C ₁ D ₂ E ₃	A ₁ B ₂ F ₁ C ₁ D ₂ E ₃
S/N ratio for kerf (db)	10.7540	11.1592

will be produced to substitute the one generated by crossover. The mutation procedure consists of replacing one of the decision variable values of an individual, while keeping the remaining variables unchanged. The replaced variable is randomly chosen, and its new value is calculated by randomly sampling within its specific range. The pseudo-code for standard genetic algorithm is presented below. Where S_a is initial population.

The standard genetic algorithm

```

{
Generate initial population. Sa
Evaluate population Sa
While stopping criteria not satisfied repeat
{
Select elements from Sa put into Sa+1
Crossover elements of Sa and put into Sa+1
Mutate elements of Sa and put into Sa+1
Evaluate new population Sa+1
Sa=Sa+1
}
}
```

A weighting factor is used to provide importance to the performance measures as per requirement of the decision-maker. Table 12 shows the optimum conditions of the machining parameters for multi-performance outputs with different combinations of the weighting factors. In this study, case-1 gives optimal machining performance with maximization of MRR and SF and minimization of kerf under equal importance of the weighting factors ($w_1=0.33$, $w_2=0.33$ and $w_3=0.33$). Case-1 is recommended because it gives maximum metal removal rate, maximum surface finish and minimum cutting width. The pattern of convergence of multi-objective function is shown in Fig. 14 for Case-1.

Table 9 Results of the confirmation experiment for SF

	Optimal machining parameter	
	Prediction	Experimental
Level	A ₃ B ₂ F ₁ C ₃ D ₂ E ₂	A ₃ B ₂ F ₁ C ₃ D ₂ E ₂
S/N ratio for SF (db)	86.75	85.06

Table 11 Genetic algorithm parameters for cases 1, 2, 3 and 4

Population size	50
Maximum number of generation	500
Number of problem variables	6
Probability of crossover	75%
Probability of mutation	5%

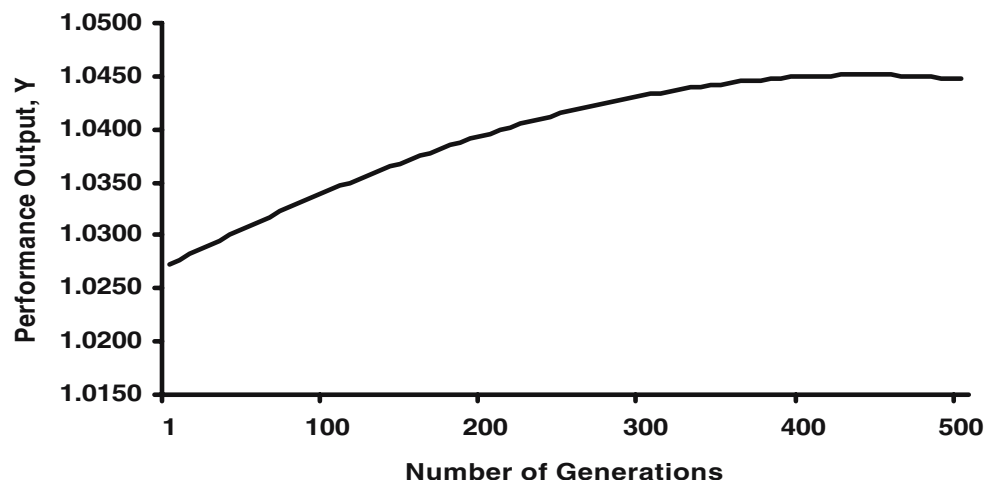
Table 12 Optimum machining conditions for multi-performance with different weighting factors

Control factors and performance measures	Optimum machining conditions			
	Case 1: ($w_1=0.33$, $w_2=0.33$ & $w_3=0.33$)	Case 2: ($w_1=0.80$, $w_2=0.10$ & $w_3=0.10$)	Case 3: ($w_1=0.10$, $w_2=0.80$ & $w_3=0.10$)	Case 4: ($w_1=0.10$, $w_2=0.10$ & $w_3=0.80$)
A: Discharge current	16.06	16.28	16.09	16.51
B: Pulse duration	3.29	12.63	3.40	3.20
C: Pulse frequency	60.00	42.30	51.36	58.14
D: Wire speed	9.03	7.82	9.09	8.53
E: Wire tension	1099	1192	1008	1067
F: Dielectric flow rate	1.38	1.29	1.36	1.39
MRR (g/min)	0.15555	0.17291	0.13318	0.13305
SF (μm)	81.5318	88.4431	81.2441	81.2481
Kerf (mm)	0.202	0.259	0.203	0.204

6 Conclusions

In this work, an attempt was made to determine the important machining parameters for performance measures like MRR, SF, and kerf separately in the WEDM process. Factors like discharge current, pulse duration, and dielectric flow rate and their interactions have been found to play a significant role in rough cutting operations for maximizations of MRR, minimization of surface roughness and minimization of cutting width. Taguchi's experimental design method is used to obtain optimum parameter combination for maximization of MRR, SF as well as minimization of kerf. Interestingly, the optimal levels of the factors for all the objectives differ widely. In order to optimize for all the three objectives, mathematical models are developed using the non-linear regression method. The confirmation experiment shows that the errors associated with MRR, SF, and

kerf are 3.14, 1.95, and 3.72%, respectively. The optimum search of machining parameter values for the objective of maximizing of MRR and SF and minimization of kerf are formulated as a multi-objective, multi-variable, non-linear optimization problem. This study also evaluates the performance measures with equal importance to weighting factors since higher MRR, SF and low kerf are equally important objectives in WEDM application. The rationale behind the use of genetic algorithm lies in the fact that genetic algorithm has the capability to find the global optimal parameters whereas the traditional optimization techniques normally stuck up at the local optimum values. The algorithm is tested to find optimal values of parameters varying weighting factors for different objectives. In future, the study can be extended using different work materials, and hybrid optimization techniques.

Fig. 14 Convergence curve

Acknowledgements The authors are extremely thankful to the referees for their valuable comments and suggestions which contributed significantly to improve the quality of the paper.

References

1. Trezise KE (1982) A physicist's view of wire EDM. Proceedings of the International Conference on Machine Tool Design and Research 23:413–419
2. Rajurkar KP, Wang WM (1993) Thermal modeling and on-line monitoring of wire-EDM. *J Mater Process Technol* 38(1–2): 417–430
3. Tarng YS, Ma SC, Chung LK (1995) Determination of optimal cutting parameters in wire electrical discharge machining. *Int J Mach Tools Manuf* 35(129):1693–1700
4. Scott D, Boyina S, Rajurkar KP (1991) Analysis and optimization of parameter combination in wire electrical discharge machining. *Int J Prod Res* 29(11):2189–2207
5. Lok YK, Lee TC (1997) Processing of advanced ceramics using the wire-cut EDM process. *J Mater Proces Technol* 63(1–3):839–843
6. Huang JT, Liao YS, Hsue WJ (1999) Determination of finish-cutting operation number and machining parameters setting in wire electrical discharge machining. *J Mater Process Technol* 87:69–81
7. Rozenek M, Kozak J, DabroVwki L, LubkoVwki K (2001) Electrical discharge machining characteristics of metal matrix composites. *J Mater Process Technol* 109:367–370
8. Tosun N, Cogun C (2003) An investigation on wire wear in WEDM. *J Mater Process Technol* 134(3):273–278
9. Tosun N, Cogun C, Pihtili H (2003) The effect of cutting parameters on wire crater sizes in wire EDM. *Int J Adv Manuf Technol* 21:857–865
10. Sho H, Orimo T, Fukui M (1989) The effect of electrode materials on the characteristics of machinability of wire electro discharge machines,. Proceedings of the International Symposium for Electro Machining (ISEM-9) Nagoya 219–222
11. Peace SG (1993) Taguchi methods: a hands on approach. Addison-Wesley, New York
12. Phadke MS (1989) Quality engineering using robust design. Prentice Hall Eaglewood Cliffs, New Jersey
13. Holland JH (1975) Adaptation in natural and artificial systems. The University of Michigan Press, Ann Arbor, Michigan